



Atmospheric new particle formation enhanced by tricarboxylic acids

Astrid Nørskov Pedersen, Yosef Knattrup, and Jonas Elm

Department of Chemistry, Aarhus University, Langelandsgade 140, 8000 Aarhus C, Denmark

Correspondence: Jonas Elm (jelm@chem.au.dk)

Abstract.

Organic molecules contribute significantly to the formation of aerosols in the atmosphere, forming what is known as secondary organic aerosols (SOA). The organic molecules are emitted as volatile organic compounds (VOCs), and undergo a number of reactions in the atmosphere. Due to the variety in both VOCs and reaction pathways, it has been difficult to elucidate the exact structure of an organic molecule that is able to drive new particle formation (NPF). We have studied the NPF ability of three different oxygenated organic molecules (OOM); 3-methyl-1,2,3-butanecarboxylic acid (MBTCA), carboxyheptanoic acid (CHA) and pinyl diaterpenylic ester (PDPE). These all contain three carboxylic acids, which previous work suggest is a good candidate for driving NPF, and have been observed in the atmosphere, as well as in lab experiments. Using computational methods, we studied the $(\text{OOM})_{1-2}(\text{SA})_{0-2}(\text{base})_{0-2}$ clusters, where SA = sulfuric acid and base = [ammonia (AM), methylamine (MA), dimethylamine (DMA) and trimethylamine (TMA)]. Geometry optimization and thermochemical parameters are calculated at the $\omega\text{B97-XD/6-31++G(d,p)}$ level of theory, and single point energies are calculated at the $\text{DLPNO-CCSD(T}_0\text{)}/\text{aug-cc-pVTZ}$ level of theory. We found that PDPE was able to produce the most stable clusters, presumably due to its high flexibility. Cluster formation potentials are simulated using the Atmospheric Cluster Dynamics Code. We found that all three OOMs were able to enhance cluster formation for the $(\text{OOM})(\text{SA})(\text{base})$ systems by 2–3 orders of magnitude for the most significant systems. Especially the $(\text{OOM})(\text{SA})(\text{DMA})$ system has a high cluster formation potential, with similar trends across all three OOMs.

1 Introduction

Atmospheric aerosols can act as cloud condensation nuclei (CCN), increasing the global albedo (Boucher and Lohmann, 1995), or scatter light themselves (Canadell et al., 2021). This is known as the indirect and direct aerosol effect, respectively, both of which have a net cooling effect on the global climate (Canadell et al., 2021). Aerosols are still responsible for the largest uncertainty in modern radiative forcing models, according to the Intergovernmental Panel on Climate Change (IPCC) (Canadell et al., 2021). Atmospheric aerosols are either directly emitted into the atmosphere as primary aerosols, or emerge through clustering of molecules initially emitted into the atmosphere as gaseous species. The latter process is known as new particle formation (NPF), and is the mechanism responsible for secondary aerosols (Kulmala et al., 2013). Usually, the gaseous species have to undergo oxidation, lowering their volatility, before NPF is favorable. On average, it is estimated that globally



about 50% of CCN arise from NPF (Boucher and Lohmann, 1995; Merikanto et al., 2009), with a higher fraction over the eastern United States and a lower fraction over mainland Europe Zhao et al. (2024).

It is well-known that inorganic acids and bases are important for the initial cluster formation over land (Kulmala et al., 2013). Some confirmed aerosol precursors are sulfuric acid (SA) (Sipilä et al., 2010), water (Loukonen et al., 2010; Temelso et al., 2012a; ; Temelso et al., 2012b; Henschel et al., 2014; Rasmussen et al., 2020; Neeffjes et al., 2026), and bases such as ammonia (AM) (Weber et al., 1996; Kirkby et al., 2011; Elm, 2021b; Dunne et al., 2016), as well as amines such as methylamine (MA), dimethylamine (DMA), and trimethylamine (TMA) (Almeida et al., 2013; Elm et al., 2020; Engsvang et al., 2023; Kurtén et al., 2008; Loukonen et al., 2010; Nadykto et al., 2011, 2015, 2014; Jen et al., 2014; Glasoe et al., 2015; Elm, 2021b, b; Kurtén et al., 2008; Nadykto et al., 2011; Jen et al., 2014; Nadykto et al., 2015; Glasoe et al., 2015). Over the oceans, it is the oxidation products of dimethylsulfide, such as methanesulfonic acid (Barnes et al., 2006), as well as various iodine species that are believed to drive NPF together with SA (O'Dowd et al., 2002; Sipilä et al., 2016; He et al., 2021, 2023). Organic molecules make up a large part of the total atmospheric aerosol load (Jimenez et al., 2009; Hallquist et al., 2009), with secondary organic aerosols (SOA) making up 15–80% by mass of global PM_{2.5} (Hallquist et al., 2009). Zhang et al. (2004) showed that aromatic acids enhance nucleation of SA, due to the formation of a complex between SA and the aromatic acid causing a lowered nucleation barrier. In addition, multiple chamber studies has proved that this is also true for oxidation products of biogenic terpenes, like α -pinene and Δ -3-carene (Hoffmann et al., 1997; Pathak et al., 2007; Laj et al., 2009; Zhang et al., 2009; Metzger et al., 2010; Schobesberger et al., 2013; Riccobono et al., 2014; Quéléver et al., 2019; Simon et al., 2020; Thomsen et al., 2021, 2022, 2024). SOA are especially important in rural sites, where the concentration of organics is high compared to the concentration of SA (Fang et al., 2020; Ehn et al., 2014) Fang et al. (2020) suggested that dicarboxylic acids take part in NPF, given that the observed nucleation rates in their field study could not be explained by SA–AM or SA–DMA clustering alone.

Clustering of organic molecules has been studied for almost 20 years using quantum chemical methods, starting with Nadykto and Yu (Nadykto and Yu, 2007), who studied the interaction between AM or water and simple, common carboxylic acids such as formic and acetic acid. More recently, larger oxygenated organic molecules, including multiple alcohol and/or carboxyl groups were studied computationally, showing binding free energies as low as -14.37 kcal/mol for dimer clusters of dicarboxylic acids (Tan et al., 2022).

Given the vast number of different volatile organic compounds (VOCs) emitted into the atmosphere and the complexity of the possible reaction pathways, the area of organic nucleation has proven to be difficult to study. (Elm et al., 2023) concluded that, despite SOA being studied extensively through many years, both experimentally and computationally, the exact structure of an organic molecule that is able to drive nucleation has not yet been identified. With the limited knowledge available, it is not yet clear whether organics are important for nucleation or only enter the particle after it has been formed, contributing to particle growth (Kulmala et al., 2013). Carboxylic acids are believed to be the most promising organic functional group to be involved in new particle formation (Elm et al., 2017). In our previous work using the cluster-of-functional-groups approach (Pedersen et al., 2024), we showed that three different formic acid molecules, representing a tricarboxylic acid, should form stable clusters with sulfuric acid and bases, where the bases are AM, MA, DMA, and TMA. Especially DMA showed increased



cluster formation rates when the concentration of oxygenated organic molecules (OOMs) were increased, due to its high base strength.

Tan et al. (2022) studied eight different organic–SA systems, and found that the carboxyheptanoic acid–SA systems, as well as the phthalic acid–SA systems, had high cluster formation potentials, suggesting that organic molecules can indeed play a role in nucleation. Large accretion products, also called dimers, are believed to be able to drive organic nucleation (Lehtipalo et al., 2018; Dada et al., 2023). These are believed to be formed by gas-phase cross reaction of two alkoxyradicals to form an accretion product (Peräkylä et al., 2023). However, Kenseth et al. (2023) argue that they can only be produced in the particle phase, leaving them unable to participate in NPF.

In this article, we study the nucleating ability of three different organic molecules, 3-methyl-1,2,3-butanecarboxylic acid (MBTCA), carboxyheptanoic acid (CHA) and pinyl diaterpenylic ester (PDPE) (see Figure 1). These have been chosen as they all contain three carboxylic acid moieties and have been observed experimentally. MBTCA is formed from OH-initiated

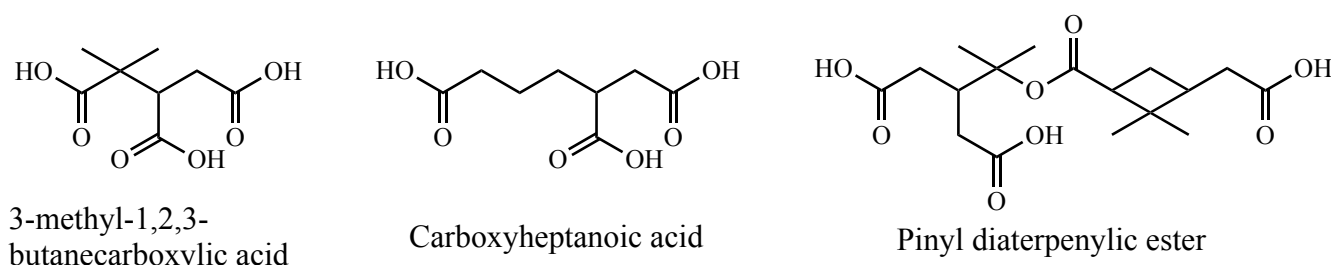


Figure 1. Structure of the three organic molecules studied.

oxidation of α -pinene, and has been observed in chamber experiments, and in field campaigns in the Sierra Nevada Mountains in California (Müller et al., 2012; Kristensen et al., 2013). PDPE, a large accretion product, was found to be formed from α -pinene oxidation using O_3 (Kristensen et al., 2016), and was also found in the same field study from the Sierra Nevada mountains (Kristensen et al., 2013), as well as in a field study in Hyytiälä, Finland (Kristensen et al., 2016). CHA was identified in a chamber experiment as a product of the photooxidation of a *d*-limonene/ NO_x /air mixture, and has also been detected in field studies in Hungary (Jaoui et al., 2006; Yasmeen et al., 2011). The clustering ability of both MBTCA and CHA has already been studied using quantum chemical techniques (Tan et al., 2022), finding that trimers made up of both SA and the organic molecule were stable enough, leading to negligible evaporation.

The clustering ability of MBTCA, CHA and PDPE is studied, both in purely organic clusters, as well as in $(SA)_{1-2}(Base)_{1-2}$ clusters, where the bases are ammonia (AM), methylamine (MA), dimethylamine (DMA) and trimethylamine (TMA). These have been shown to enhance nucleation in clusters containing sulfuric acid (Kulmala et al., 2013; Kirkby et al., 2011; Schobesberger et al., 2013; Weber et al., 1996; Dunne et al., 2016; Almeida et al., 2013; Elm et al., 2020; Engsvang et al., 2023; Kurtén et al., 2008; Loukonen et al., 2010; Nadykto et al., 2011, 2015, 2014; Jen et al., 2014; Glasoe et al., 2015; Elm, 2021b). This was done by calculating the binding Gibbs free energy at the DLPNO-CCSD(T_0)/aug-cc-pVTZ// ω B97X-D/6-31++G(d,p) level of theory using an extensive configurational sampling workflow to find the global free energy minimum structure. The



thermodynamic data was used as input in the Atmospheric Cluster Dynamics Code (ACDC) to calculate cluster formation rates for the $(SA)_{1-2}(Base)_{1-2}(OOM)_{1-2}$ systems.

2 Methods

90 2.1 Computational details

ABCluster (Zhang and Dolg, 2015) was used for initial configurational search with the CHARMM forcefield, using population size, $SN = 3000$, maximum generations, $g_{max} = 200$, and number of scout bees, $g_{limit} = 4$, as recommended by Kubečka et al. (2019). A total of 1000 local minima were saved for each protonation state. Semi-empirical GFN1-xTB energy calculations and geometry optimizations were executed using the XTB 6.4.0 program (Grimme et al., 2017). Further search of the potential
95 energy surface (PES) was performed using CREST 2.12 (Pracht et al., 2020) at GFN1-xTB level within the iterative metadynamics genetic structure crossing (iMTD-GC) workflow. An energy window of 30 kcal mol^{-1} was used, accounting for the fact that the potential energy surface (PES) at the semi-empirical level is not necessarily parallel to the PES at higher levels of theory. DFT calculations with the ω B97X-D functional (Chai and Martin, 2008) and 6-31++G(d,p) basis set were performed using Gaussian16, version B.01 (Gau), using default convergence criteria. DLPNO-CCSD(T_0) (Riplinger and Neese, 2013;
100 Riplinger et al., 2013) single point energies were calculated in ORCA 5.0.4 (ORC; Neese, 2022), with the aug-cc-pVTZ basis set, using the TightSCF convergence criteria and the NormalPNO setting (Liakos et al., 2015). Both the workflow and data processing were automated with JKCS (Kubečka et al., 2023a).

2.2 Configurational sampling workflow

For the configurational search, a funnel-type procedure was employed (Temelso et al., 2018; Odbadrakh et al., 2020; Kubečka
105 et al., 2023a), where the level of theory is increased as the number of cluster candidates is decreased;

ABCluster \rightarrow GFN1-xTB \rightarrow CREST \rightarrow ω B97X-D \rightarrow DLPNO.

The initial cluster structures were generated using ABCluster. These were optimized using GFN1-xTB. The structure with the lowest electronic energy at this level was used as input for additional configuration sampling using CREST, which accommodated internal rotations of bonds for flexible molecules when searching the PES. The 100 cluster structures with the lowest
110 electronic energy after the CREST calculation were selected to be optimized at the DFT-level. Single point energies using DLPNO-CCSD(T_0)/aug-cc-pVTZ were calculated for the five clusters with the lowest electronic energy at the DFT-level.

2.3 Atmospheric cluster dynamics code

The ACDC workflow (McGrath et al., 2012) generates and solves the birth-death equations, giving the change in concentration of cluster i as a function of condensation and evaporation,

$$115 \frac{dc_i}{dt} = \sum_{j < i} \beta_{j,(i-j)} c_j c_{(i-j)} + \sum_j \gamma_{(i+j) \rightarrow i} c_{(i+j)} - \sum_j \beta_{i,j} c_i c_j - \sum_{j < i} \gamma_{i \rightarrow j} c_i + Q_i - S_i. \quad (1)$$



where j is another cluster or monomer in the system, $\beta_{i,j}$ is the collision coefficient between cluster i and j , $\gamma_{i \rightarrow j}$ is the evaporation coefficient of cluster i into smaller clusters, one of which is cluster j . Q_i covers outside sources of i , and S_i other possible loss mechanisms for i . The collision coefficient is given by kinetic gas theory and the evaporation coefficient is given by mass balance based on the calculated Gibbs free energy,

$$120 \quad \gamma_{(i+j) \rightarrow i} = \beta_{i,j} c_{\text{ref}} \exp\left(\frac{\Delta G_{i+j} - \Delta G_i - \Delta G_j}{k_{\text{B}} T}\right), \quad (2)$$

where c_{ref} is the reference pressure (1 atm).

Due to computational limitations, it is not possible to simulate the cluster formation all the way from gas species to fully stable particles. Therefore, a limit has been chosen where the clusters are assumed to be stable against evaporation and are counted towards the cluster formation rate. These clusters will be referred to as "outgrowing". In this study, we explicitly
125 calculated thermodynamic data for the SA–OOM–Base clusters up to size $2 \times 2 \times 2$, while the data for the SA–Base clusters up to size 3×3 was obtained from Kubečka et al. (2023b). The outgrowing clusters are therefore chosen to be (SA)₄(base)₃, (SA)₃(OOM)₂(base)₂, (SA)₂(OOM)₃(base)₂ and (SA)₃(OOM)₁(base)₃. Given that these outgrowing clusters are fairly small, the systems are artificially stable, and the critical cluster size may not yet have been reached, meaning the calculated formation rates are overestimated. In order to distinguish the calculated rates from actual nucleation rates, we denote them as cluster
130 formation potentials ($J_{\text{potential}}$), as they represent the potential of clusters to grow to larger sizes, and should be interpreted as an upper limit to the nucleation rate. A more in-depth discussion of cluster formation potentials is given in Clusteromics I (Elm, 2021b). Finally, we defined the main outgrowing paths as the pathway following the highest flux backwards from the outgrowing clusters toward the monomers.

3 Results and discussion

135 3.1 Cluster Thermochemistry

The limiting step in atmospheric cluster formation is often the formation of the initial dimer cluster (Olenius et al., 2013; Elm et al., 2017). Usually, organics bind too weakly to themselves and sulfuric acid to initiate the initial dimer cluster formation. The calculated binding Gibbs free energies of the three purely organic dimer clusters, (MBTCA)₂, (CHA)₂, and (PDPE)₂, are given in Table 1. The (SA)₁(DMA)₁ cluster is included as reference, because this system has been studied extensively, and
140 shown to form stable clusters (Kurtén et al., 2008; Kubečka, 2021).

The MBTCA–MBTCA and CHA–CHA interactions are both slightly weaker than the SA–DMA interaction, but the difference is very small. The PDPE–PDPE interaction is the strongest, even stronger than the SA–DMA interaction, suggesting a high probability for PDPE to drive NPF. Organic clusters have been extensively studied in the literature, with much emphasis on di/tri-carboxylic acids. For instance, Elm et al. (2019) studied 13 dicarboxylic acid dimer clusters at the same level of theory as
145 used in this study. They found that the glutaric acid (5 carbon backbone) dimer has a binding free energy of $-11.6 \text{ kcal mol}^{-1}$, suberic acid (6 carbon backbone) dimer cluster has a binding Gibbs free energy of $-9.9 \text{ kcal mol}^{-1}$, and the pimelic acid (7



Cluster	Binding Gibbs Free Energy (kcal mol ⁻¹)
(SA) ₁ (DMA) ₁	-12.82
(MBTCA) ₂	-9.96
(CHA) ₂	-11.62
(PDPE) ₂	-13.52

Table 1. The binding free energy (in kcal/mol), at the DLPNO-CCSD(T₀)/aug-cc-pVTZ// ω B97X-D/6-31++G(d,p) level of theory with quasi-harmonic cutoff of 100 cm⁻¹, calculated at 298.15 K and 1 atm, of the (OOM)₂ clusters.

carbon backbone) dimer has a binding free energy of -13.0 kcal mol⁻¹, while the rest of the dimer clusters they studied had significantly higher binding free energies.

150 Other dicarboxylic acids originating from biogenic sources have been studied. For the pinic acid dimer cluster (Elm et al., 2014), a binding Gibbs free energy of -7.05 kcal mol⁻¹ was found, calculated at the M06-2X/6-311++G(3df,3pd) level of theory. Malonic acid (MOA)₂ yields $\Delta G = -8.29$ kcal mol⁻¹ with the RI-MP2/cc-pVTZ//PW91PW91/6-311++G(2d,2p) level of theory (Wang et al., 2021) or $\Delta G = -4.35$ kcal mol⁻¹ at the M06-2X/6-311++G(3df,3pd) level of theory (Zhang et al., 2018). This illustrates that the applied level of theory has a major impact on the modeled values and one have to be cautious, especially with the applied single point energy. While some of the previously studied dicarboxylic acids rival the binding free energy values of the tricarboxylic acids in Table 1, they also lead to “dead-end” closed structures where there is no place for more molecules to attach. In order to facilitate cluster formation the organics need to bind strong enough to the initial cluster, as well as enhance the attachment of additional molecules to the cluster.

155

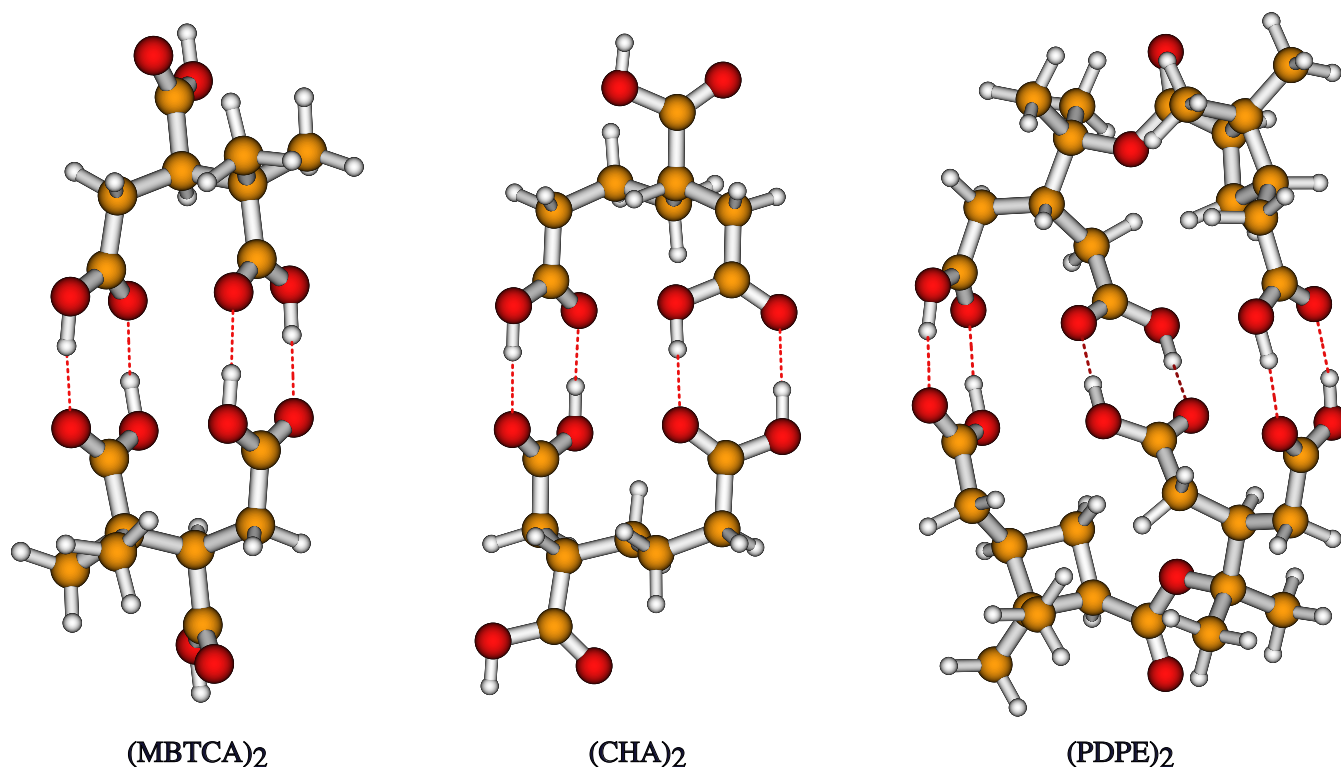


Figure 2. The (OOM)₂ cluster geometries lowest in free energy at the DLPNO-CCSD(T₀)/aug-cc-pVTZ// ω B97X-D/6-31++G(d,p) level of theory with a quasi-harmonic threshold of 100 cm⁻¹, at 298.15 K and 1 atm. Orange is carbon, red is oxygen, and white is hydrogen.

In Figure 2, the cluster geometries of the three (OOM)₂ clusters is shown. Here it can be seen that the short carbon backbone in both MBTCA and CHA restricts their ability to form three carboxylic acid–carboxylic acid bonds in the dimer clusters. (CHA)₂ is more stable than (MBTCA)₂ due to its less branched, and therefore longer, carbon backbone. This is also consistent with the study of dicarboxylic acids by Elm et al. (2019) where suberic acid dimers (7 carbon backbone) was more stable than glutaric acid dimers (5 carbon backbone). In (MBTCA)₂, the two carboxylic acid pairs are placed closer together, lowering its stability. (PDPE)₂, on the other hand, has three carboxylic acid pairs, fully utilizing its hydrogen bonding potential. This does mean that there is no obvious places for growth, and expanding the cluster would therefore involve some restructuring. The (MBTCA)₂ and (CHA)₂ clusters will more easily be able to grow, without major change in their geometry, due to the two unbound carboxylic acids in each cluster. However, introducing other nucleation precursors into the clusters might change their structure.

Given that the acid–base interaction between sulfuric acid and ammonia (Kirkby et al., 2011) or amines (Almeida et al., 2013; Elm, 2021b) is known to produce clusters, all combinations of (SA)_{1–2}(Base)_{1–2}(OOM)_{1–2} were also studied. The calculated binding Gibbs free energies of the (SA)_{1–2}(Base)_{1–2}(OOM)₁ clusters are given in Figure 3.

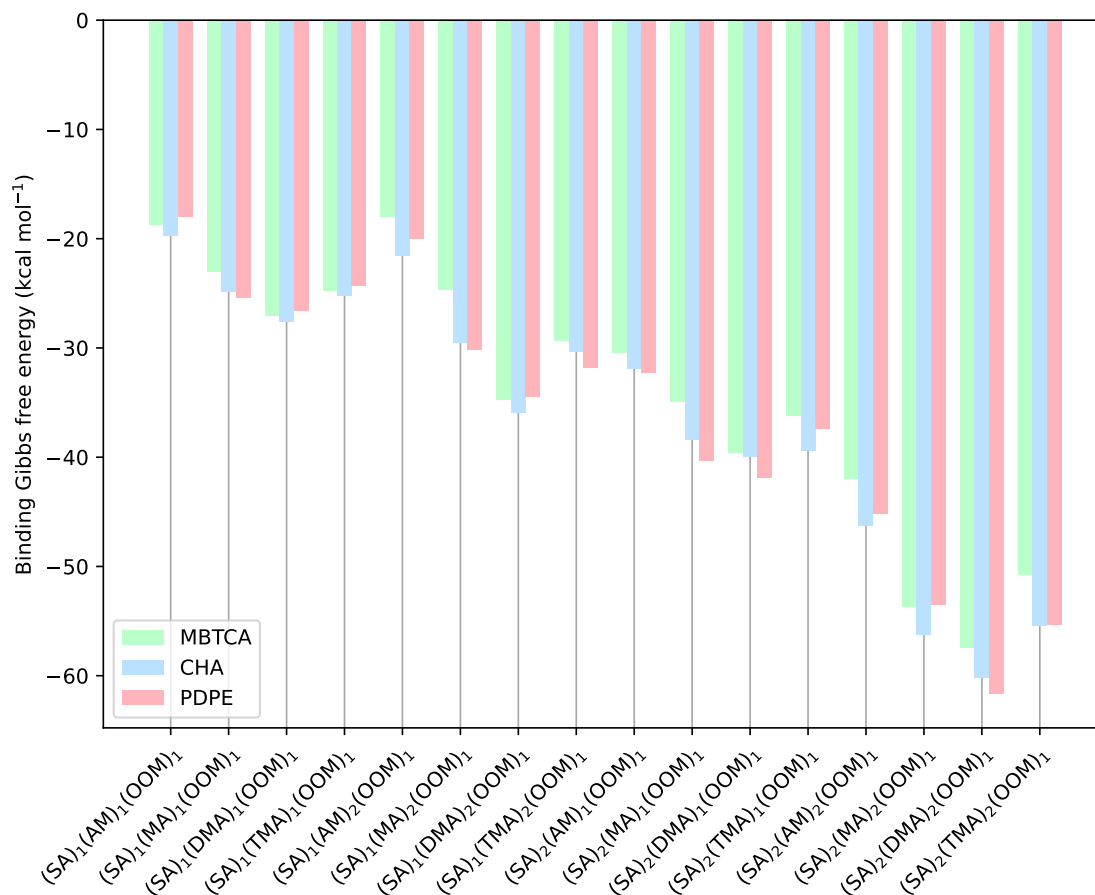


Figure 3. The binding free energy of the $(SA)_{1-2}(Base)_{1-2}(MBTCA)_1$, $(SA)_{1-2}(Base)_{1-2}(CHA)_1$ and $(SA)_{1-2}(Base)_{1-2}(PDPE)_1$ clusters, calculated at the DLPNO-CCSD(T_0)/aug-cc-pVTZ// ω B97X-D/6-31++G(d,p) level of theory with a quasi-harmonic threshold of 100 cm^{-1} , at 298.15 K and 1 atm.

Not surprisingly, the overall trend shows that the addition of more SA and base both act to lower the binding Gibbs free energy of the clusters. This is in accordance with what was previously seen when the OOMs were represented by three formic acid molecules (Pedersen et al., 2024). Similar to the pure organic dimers, PDPE was again able to produce the most stable cluster. Overall, PDPE is only the strongest binding OOM in 7 out of the 16 clusters, with CHA being the strongest binding OOM in the remaining clusters. **Within all cluster sizes, and across all OOMs, DMA is the strongest binding base.**

For the smallest clusters, PDPE is generally unfavorable. This could be due to its large size and high flexibility, that makes it able to position the carboxylic acid groups in the most favorable positions, but introduces more steric hindrance for the



180 smaller clusters. The $(SA)_1(DMA)_1(OOM)_1$ and $(SA)_2(DMA)_2(OOM)_1$ clusters are shown in Figure 4. As can be seen in
185 Figure 4, both MBTCA and CHA have an available carboxylic acid group in the $(SA)_1(DMA)_1(OOM)_1$ clusters, while the
larger PDPE molecule is able to make use of all three carboxylic acid groups when interacting with the sulfuric acid and bases.
However, as stated above, this cluster is 1 kcal mol^{-1} less stable than the $(SA)_1(DMA)_1(CHA)_1$ cluster, due to steric hindrance
introduced by the large PDPE molecule. In the $(SA)_2(DMA)_2(OOM)_1$ clusters, all three OOMs have three binding carboxyl
groups. This means that PDPE is able to stretch out, minimizing the steric hindrance while maximizing the number of favorable
interactions yielding a binding Gibbs free energy of $-61.7 \text{ kcal mol}^{-1}$. For the $(SA)_2(DMA)_2(MBTCA)_1$ ($-57.4 \text{ kcal mol}^{-1}$)
and $(SA)_2(DMA)_2(CHA)_1$ ($-60.1 \text{ kcal mol}^{-1}$) clusters, the smaller OOM means the inorganic acids and bases are closer
together to facilitate hydrogen bonding, which increases steric hindrance compared to the $(SA)_2(DMA)_2(PDPE)_1$ cluster.

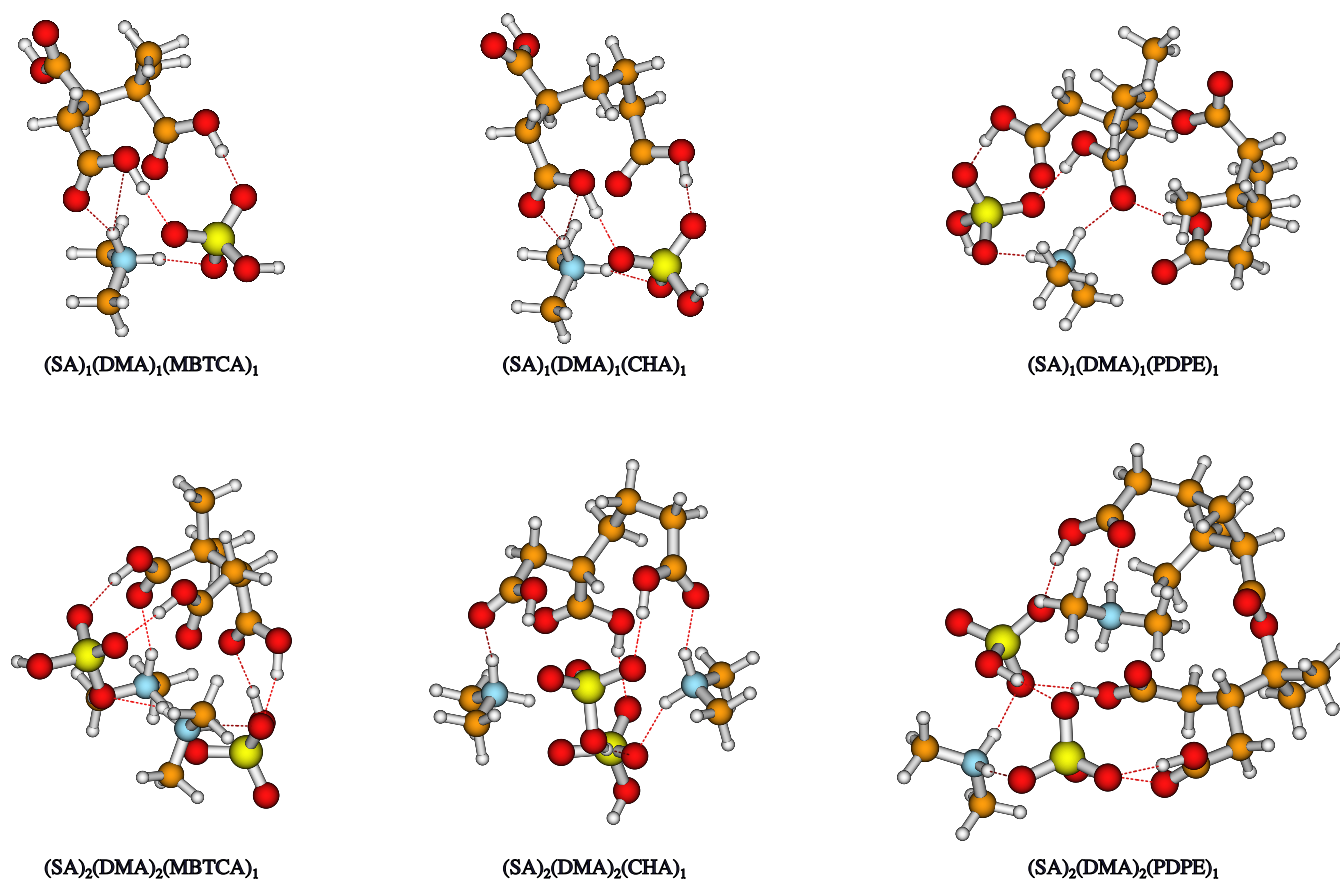


Figure 4. The $(SA)_1(DMA)_1(OOM)_1$ and $(SA)_2(DMA)_2(OOM)_1$ cluster geometries lowest in free energy at the DLPNO-CCSD(T_0)/aug-cc-pVTZ// ω B97X-D/6-31++G(d,p) level of theory with a quasi-harmonic threshold of 100 cm^{-1} , at 298.15 K and 1 atm. Orange is carbon, red is oxygen, blue is nitrogen, yellow is sulfur, and white is hydrogen.

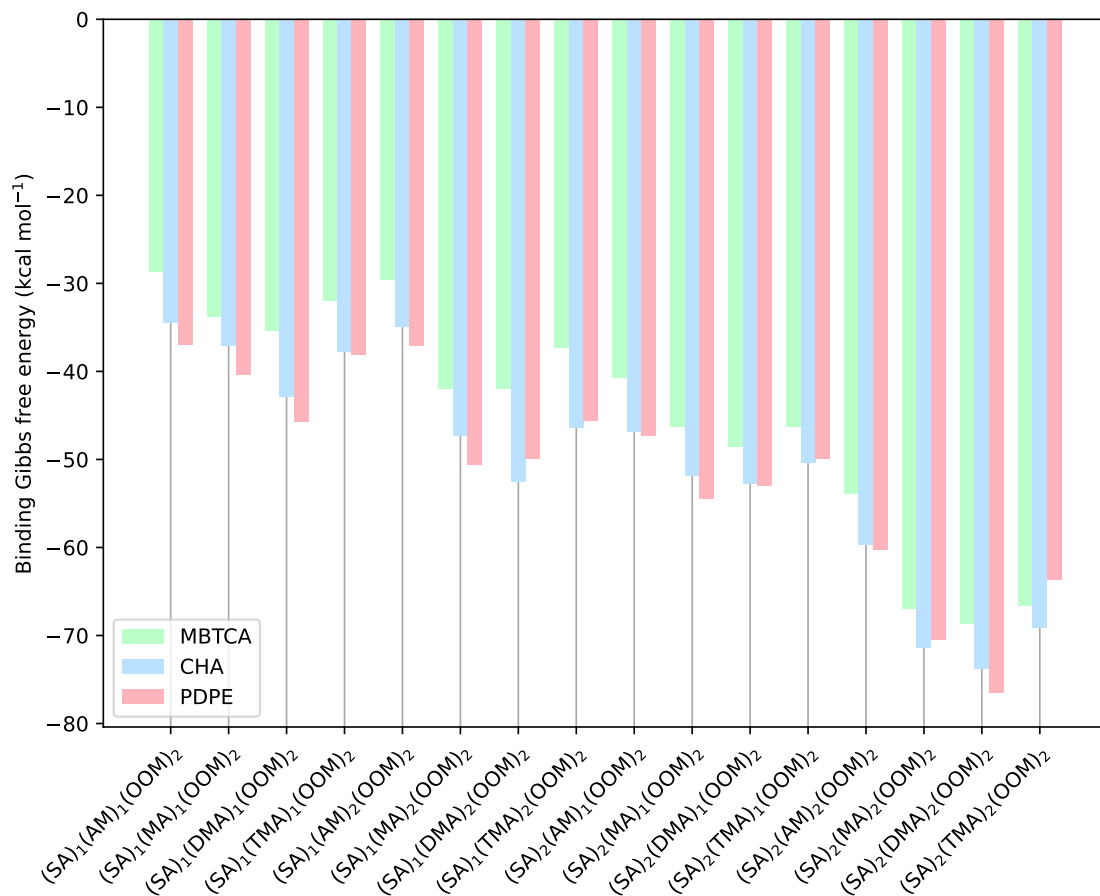


Figure 5. The binding free energy of the $(SA)_{1-2}(Base)_{1-2}(MBTCA)_2$, $(SA)_{1-2}(Base)_{1-2}(CHA)_2$ and $(SA)_{1-2}(Base)_{1-2}(PDPE)_2$ clusters, calculated at the DLPNO-CCSD(T_0)/aug-cc-pVTZ// ω B97X-D/6-31+G(d,p) level of theory with quasi-harmonic cutoff of 100 cm^{-1} , at 298.15 K and 1 atm .

The calculated binding Gibbs free energies of the $(SA)_{1-2}(Base)_{1-2}(OOM)_2$ clusters are given in Figure 5. With the addition of one more OOM, the trends remain roughly the same, with a $\sim 15\text{ kcal mol}^{-1}$ decrease in free energy across all clusters. However, DMA is no longer the strongest binding base across the board. For example, the $(SA)_1(MA)_2(PDPE)_2$ cluster has a binding Gibbs free energy of $-50.6\text{ kcal mol}^{-1}$, while the $(SA)_1(DMA)_2(PDPE)_2$ cluster has a binding Gibbs free energy of $-50.0\text{ kcal mol}^{-1}$. Generally, PDPE has been able to take advantage of how strongly it binds to itself, as PDPE is the strongest binding OOM in 11 out of the 16 clusters with two OOMs. For the remaining clusters, CHA is the strongest binding OOM, while MBTCA is the weakest binding OOM for all clusters, as was the case for the clusters with one OOM.

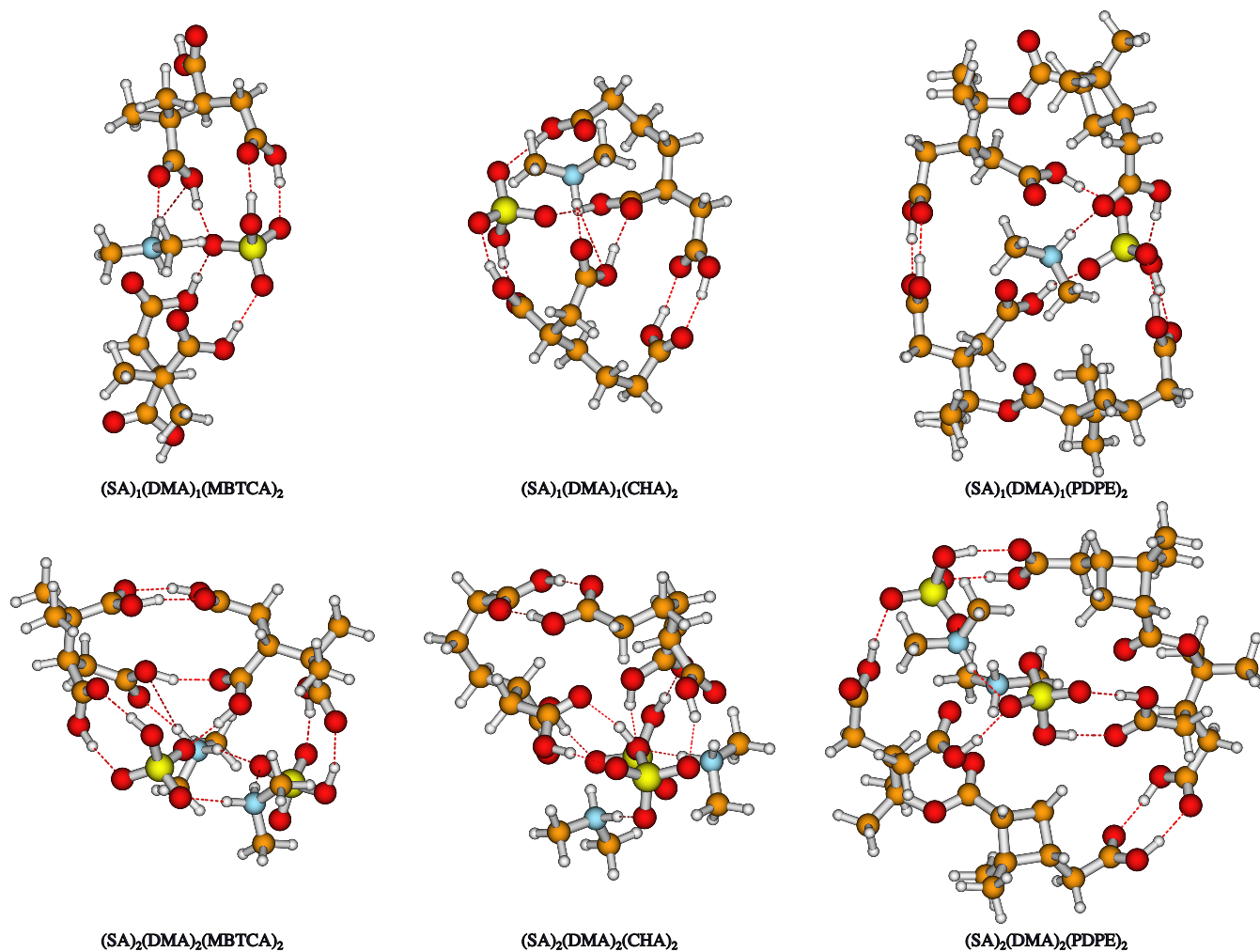


Figure 6. The (SA)₁(DMA)₁(OOM)₂ and (SA)₂(DMA)₂(OOM)₂ cluster geometries lowest in free energy at the DLPNO-CCSD(T₀)/aug-cc-pVTZ// ω B97X-D/6-31++G(d,p) level of theory with a quasi-harmonic threshold of 100 cm⁻¹, at 298.15 K and 1 atm. Orange is carbon, red is oxygen, blue is nitrogen, yellow is sulfur, and white is hydrogen.

195 The (SA)₁(DMA)₁(OOM)₂ and (SA)₂(DMA)₂(OOM)₂ clusters are shown in Figure 6, as DMA was the most favorable base for these cluster sizes. In both cases, PDPE is the most favorable OOM. As seen in Figure 6, the two clusters with PDPE are quite symmetrical, with the two PDPE molecules enclosing a core consisting of the inorganic acids and bases. Although these look close to being spherical particle-like, these cluster structures are very flat, missing the depth to fully be considered a particle. For the two clusters with CHA, it is evident that the carbon backbone on CHA is not long enough to reproduce this shell structure, instead the inorganic acids and bases is pushed to one side of the cluster instead. This is especially noticeable in the (SA)₂(DMA)₂(CHA)₂ cluster, and can also be seen in the (SA)₂(DMA)₂(MBTCA)₂ cluster. For the (SA)₁(DMA)₁(MBTCA)₂ cluster, the inorganic acid and base is sandwiched between the two MBTCA molecules, which means that two carboxylic acid

200



groups remain unbound. This results in a cluster that is noticeably less stable ($-35.3 \text{ kcal mol}^{-1}$) than the $(\text{SA})_1(\text{DMA})_1(\text{CHA})_2$ ($-42.9 \text{ kcal mol}^{-1}$) and $(\text{SA})_1(\text{DMA})_1(\text{PDPE})_2$ ($-45.8 \text{ kcal mol}^{-1}$) clusters.

205 3.2 Cluster formation potentials

From the thermochemical data in Section 3.1, we can calculate how the three OOMs: CHA, MBTCA, and PDPE, likely can stabilize a SA–base cluster. The simulated formation potentials ($J_{\text{potential}}$) of the $(\text{SA})_{1-2}(\text{base})_{1-2}(\text{OOM})_{1-2}$ systems, with base = AM, MA, DMA and TMA, and OOM = CHA, MBTCA, PDPE are given in figure 7–9. To allow for direct comparison, the vapor concentrations used are the same as those in the Clusteromics I–V series of papers (Elm, 2021b, a, 2022; Knattrup and
210 Elm, 2022; Ayoubi et al., 2023), and in the **original "cluster-of-functional-groups" paper** (Pedersen et al., 2024). The sulfuric acid concentration was fixed at $10^6 \text{ molecules cm}^{-3}$, the OOM concentration varied from 0–10 ppt, and the concentration of the bases were studied for two extremes with a “lower limit” and an “upper limit”. These were set as follows: AM (10 ppt, 10 ppb), MA (1 ppt, 100 ppt), and DMA/TMA (1 ppt, 10 ppt), with the low concentration limit likely best representing the actual concentrations observed in the ambient atmosphere. The simulations were performed at 278.15 K and 1 atm using the settings
215 described in Section 2.3.

Given that, for the OOMs, only the density of MBTCA was available in the literature, the effect of changing density was **tested on the system yielding the highest nucleation rates** (10 ppt PDPE, $[\text{SA}] = 10^6 \text{ molecules cm}^{-3}$ and 10 ppt DMA). When the density was set to that of agaric acid, a tricarboxylic acid with a relatively low density of 1.115 g cm^{-3} , the cluster formation potential was $260.71 \text{ cm}^{-3} \text{ s}^{-1}$. When the density was set to that of citric acid, another tricarboxylic acid, but with
220 a relatively high density of 1.665 g cm^{-3} , the cluster formation potential was $206.54 \text{ cm}^{-3} \text{ s}^{-1}$. **Thus, the change in density is insignificant relative to other error sources,** and the density for all three molecules was set to that of MBTCA, 1.430 g cm^{-3} (Kostenidou et al., 2018).

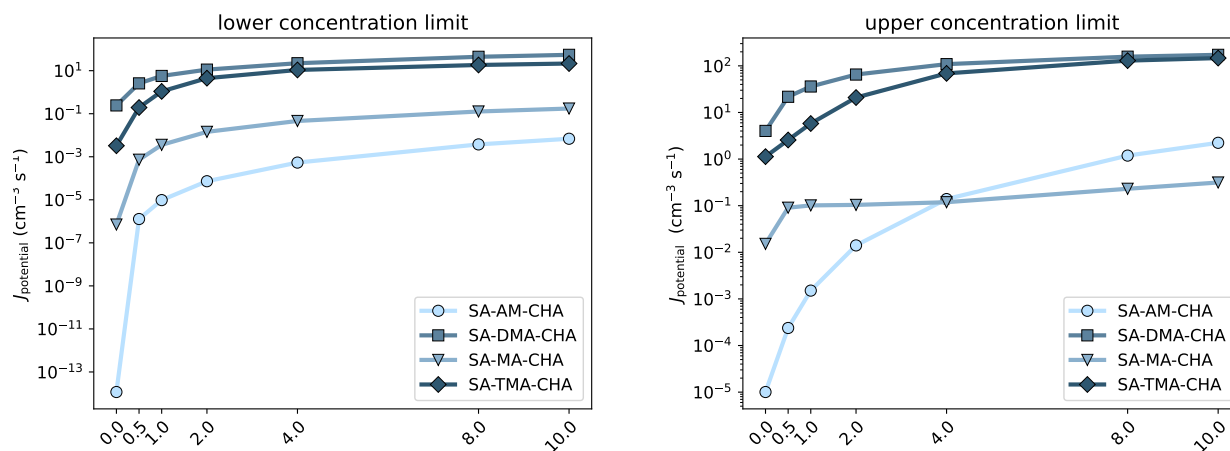


Figure 7. Simulated cluster formation potentials (in clusters $\text{cm}^{-3} \text{ s}^{-1}$) as a function of CHA mixing ratio, in the lower concentration limit (*left*) and upper concentration limit (*right*). The simulations are performed at 278.15 K and 1 atm.

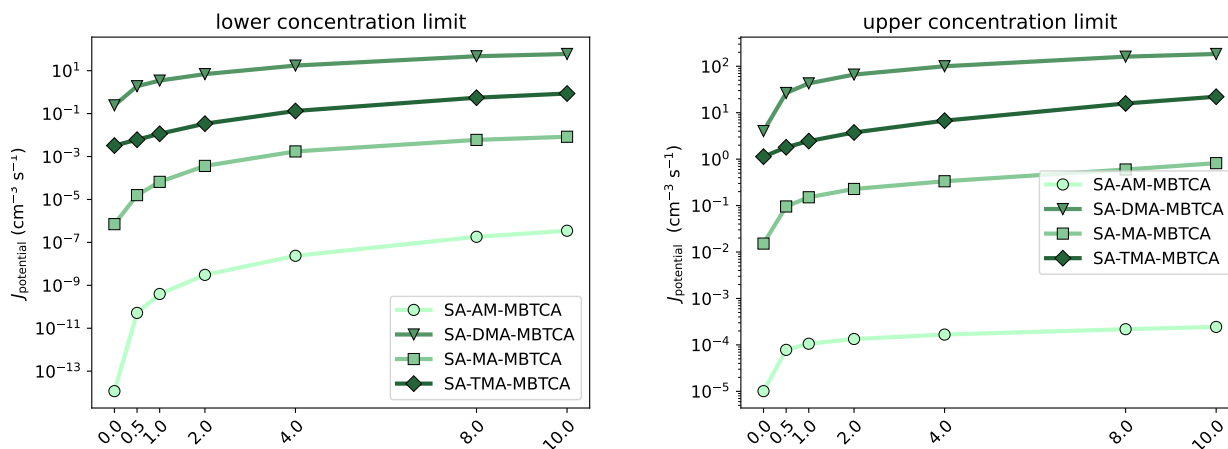


Figure 8. Simulated cluster formation potentials (in clusters $\text{cm}^{-3} \text{s}^{-1}$) as a function of MBTCA mixing ratio, in the lower concentration limit (*left*) and upper concentration limit (*right*). The simulations are performed at 278.15 K and 1 atm.

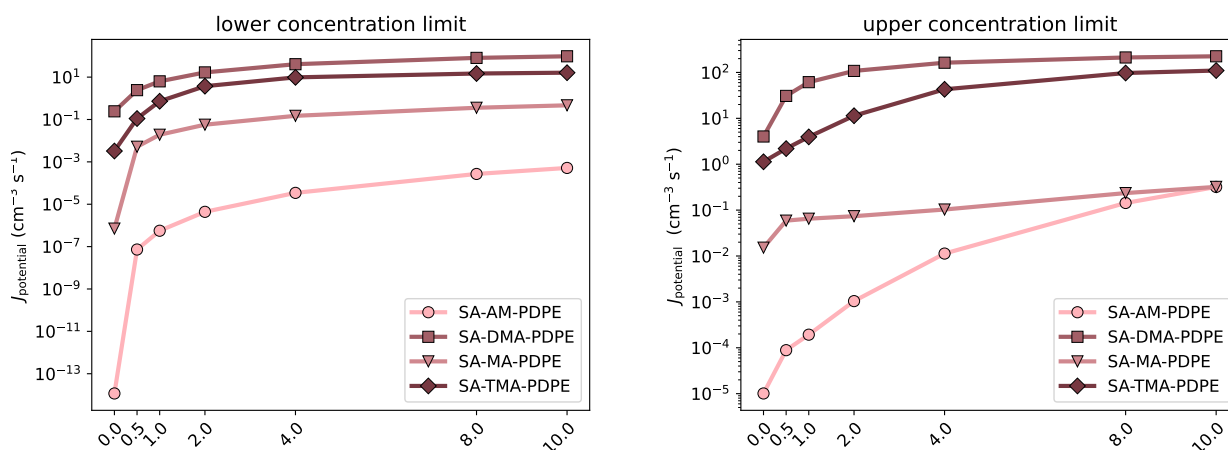


Figure 9. Simulated cluster formation potentials (in clusters $\text{cm}^{-3} \text{s}^{-1}$) as a function of PDPE mixing ratio, in the lower concentration limit (*left*) and upper concentration limit (*right*). The simulations are performed at 278.15 K and 1 atm.

225

Across all three OOMs, the trends are very similar, showing an increase in cluster formation potential as the OOM concentration increases, indicating that OOM enhances the nucleation rate. This is as expected, since the OOM lowers the binding energy sufficiently to enhance the cluster formation potential, and introducing more OOM will give more potential for binding, leading to more particles. However, the extent of this enhancement is largely dependent on the specific base in the SA–base–
 230 OOM system, and to some extent also dependent on the base concentration, as was also evident in our previous work (Pedersen et al., 2024). The largest enhancement is seen in the SA–AM–OOM systems, especially those in the lower concentration limit. We hypothesize that this is due to the weak interaction between SA and AM, meaning the OOM has a relatively large stabi-



lizing effect on the cluster, as it is otherwise weakly bound. However, since the increase in the formation potential is of the magnitude of 10^{-14} to 10^{-7} , 10^{-3} , and 10^{-4} for the SA–AM–MBTCA, SA–AM–CHA, and SA–AM–PDPE, respectively, the formation potentials for these systems are still negligible in all cases.

In agreement with the thermochemical data, the systems with the largest formation potentials are the SA–DMA–OOM systems. Interestingly, the specific OOM does not have a noticeable impact on the cluster formation potentials of these systems, with the $J_{\text{potential}}$ -value increasing 2 orders of magnitude from 1 to 10^2 the upper concentration regime, and from 10^{-1} to 10^1 in the lower concentration regime. This is in agreement with the calculated cluster formation potentials in our previous work using the the "cluster-of-functional-groups" approach (Pedersen et al., 2024). This highlights the importance of the explicit functional groups, rather than the specific molecule itself, thus validating the suitability of the "cluster-of-functional-groups" approach. This could also indicate that it might be possible to lump the compounds into groups based on their constituent functional groups. However, for the remaining bases, the trends are not as identical across the three OOMs as they are for the SA–DMA–OOM system. While the majority of the systems follow the formation potential trend of DMA>TMA>MA>AM, the SA–base–CHA system at the upper concentration limit has the formation potential of the SA–AM–CHA system overtaking that of SA–MA–CHA at a CHA concentration of 4.0 ppt. Similarly, the formation potential of the SA–AM–PDPE system catches up to that of SA–MA–PDPE at a PDPE concentration of 10 ppt. This is also very similar to the results from the "cluster-of-functional-groups" approach (Pedersen et al., 2024). This illustrates that the "cluster-of-functional-groups" approach can be used in the future to identify more complex multifunctional HOMs that could potentially contribute to NPE.

Examining the fluxes reveals that OOMs are present in all outgrowing clusters. For all systems where the base is either AM, MA, or DMA, the OOM contributes to over 90% of the outgrowing clusters. This was also the case for the SA–TMA–CHA and the SA–TMA–PDPE system in the lower concentration regime. However, at 0.5 ppt in the high base concentration regime, CHA contributes 51.67% to the outgrowing clusters, while PDPE contributes 44.33%, and MBTCA only contributes 38.44%. MBTCA also had a low contribution of only 45.46% to the outgrowing clusters at 0.5 ppt in the low base concentration regime. This low contribution of OOM to the SA–TMA–OOM clusters is caused by the strong SA–TMA interaction, as well as the bulky TMA molecule hindering the binding of the OOM to the cluster due to steric hindrance. MBTCA is the most branched, and therefore also the most rigid, of the three OOMs studied, amplifying the effect of the steric hindrance.

4 Conclusions

Based on previous results using the "cluster-of-functional-groups" approach, we were able to identify three different oxygenated organic molecules (OOMs) 3-methyl-1,2,3-butanecarboxylic acid (MBTCA), carboxyheptanoic acid (CHA) and pinyl diaterpenylic ester (PDPE), that we believe are able to form thermodynamically stable clusters in the atmosphere with sulfuric acid and nitrogen-containing bases, due to each of them containing three carboxyl groups. Using quantum chemical calculations, we studied the intermolecular interactions between the OOMs and SA–base clusters, and used the thermochemical data to study the cluster formation potentials of SA–base–OOM clusters. We find that all three OOMs are present in the most important outgrowing clusters, and that the trends across all three OOMs are similar, especially in the SA–DMA–OOM systems,



which also had the highest cluster formation potentials. This aids in proving the reliability of the “cluster-of-functional-groups” approach, as these results suggests that the functional groups, rather than the organic molecule itself, is important for cluster formation and growth.

270 The purely organic dimers were found to be fairly stable. The (PDPE)₂ cluster was more stable than the (SA)₁(DMA)₁ cluster, while the (CHA)₂ cluster was only slightly less stable. The introduction of SA and base lowered the binding Gibbs free energy significantly for all three OOMs. Given that these mixed organic and inorganic clusters are larger than the purely organic clusters studied, extending the study up to (OOM)_{3–4} may reveal that organics can form stable clusters without the need for inorganic acids and bases.

275 The data from this work can be used to gauge the accuracy of the “cluster-of-functional-groups” approach, for example, by directly comparing the binding Gibbs free energies of the clusters studied in this paper with the (SA)_{1–2}(Base)_{1–2}(Carboxylic Acid)₃ clusters from “cluster-of-functional-groups”. Assessing the accuracy of the approach will allow us to apply it for more complex multi-functional highly oxygenated molecules (HOMs) in the future.

280 *Data availability.* All the calculated structures and thermochemistry are available in the Atmospheric Cluster Database (ACDB) at: <https://github.com/elmjonas/ACDB/> (Kubečka, 2021; Elm, 2019). The datasets for this work can be found under the Articles/pedersen26_organics folder.

Author contributions. Conceptualization: J.E.;
Methodology: A.N.P, Y.K., J.E.;
Formal analysis: A.N.P, Y.K.;
Investigation: A.N.P, Y.K.;
285 Resources: J.E.;
Writing - original draft: A.N.P, Y.K., J.E.;
Writing - review & editing: A.N.P, Y.K., J.E.;
Visualization: A.N.P, Y.K.;
Project administration: J.E.;
290 Funding acquisition: J.E.;
Supervision: J.E.

Competing interests. J.E is a member of the Editorial Board of Aerosol Research. The remaining authors have no conflict of interests to declare.



295 *Acknowledgements.* This work was funded by the Danish National Research Foundation (DNRF172) through the Center of Excellence for Chemistry of Clouds.

The numerical results presented in this work were obtained at the Centre for Scientific Computing, Aarhus <https://phys.au.dk/forskning/faciliteter/cscaa/>.

The authors thank Professor Merete Bilde for insightful discussions of the work.



References

300

Gaussian 16, Revision A.03, M. J. Frisch, G. W. Trucks, H. B. Schlegel, G. E. Scuseria, M. A. Robb, J. R. Cheeseman, G. Scalmani, V. Barone, G. A. Petersson, H. Nakatsuji, et al., Gaussian, Inc., Wallingford CT, 2016.

Neese F., WIREs Comput. Mol. Sci. 2012, 2: 73–78 doi: 10.1002/wcms.81.

Almeida, J., Schobesberger, S., Kürten, A., Ortega, I. K., Kupiainen-Määttä, O., Praplan, A. P., Adamov, A., Amorim, A., Bianchi, F.,
305 Breitenlechner, M., and et al.: Molecular Understanding of Sulphuric Acid-Amine Particle Nucleation in the Atmosphere, *Nature*, 502, 359–363, <https://doi.org/10.1038/nature12663>, 2013.

Ayoubi, D., Knattrup, Y., and Elm, J.: Clusteromics V: Organic Enhanced Atmospheric Cluster Formation, *ACS Omega*, 8, 9621–9629, 2023.

Barnes, I., Hjorth, J., and Mihalopoulos, N.: Dimethyl Sulfide and Dimethyl Sulfoxide and Their Oxidation in the Atmosphere, *Chem. Rev.*, 106, 940–975, 2006.

310 Boucher, O. and Lohmann, U.: The Sulfate-CCN-Cloud Albedo Effect, *Tellus B: Chem. Phys. Meteorol.*, pp. 281–300, <https://www.tandfonline.com/doi/abs/10.3402/tellusb.v47i3.16048>, 1995.

Canadell, J. G., Monteiro, P. M. S., Costa, M. H., Cotrim da Cunha, L., Cox, P., Eliseev, A. V., Henson, S., Ishii, M., Jaccard, S., Koven, C., and et al.: Global Carbon and other Biogeochemical Cycles and Feedbacks, pp. 673–816, Cambridge University Press, Cambridge, United Kingdom and New York, NY, USA, 2021.

315 Chai, J. and Martin, H.: Long-Range Corrected Hybrid Density Functionals with Damped Atom-Atom Dispersion Corrections, *Phys. Chem. Chem. Phys.*, 10, 6615–6620, 2008.

Dada, L., Stolzenburg, D., Simon, M., Fischer, L., Heinritzi, M., Wang, M., Xiao, M., Vogel, A. L., Ahonen, L., Amorim, A., et al.: Role of Sesquiterpenes in Biogenic New Particle Formation, *Sci. Adv.*, 9, eadi5297, 2023.

Dunne, E. M., Gordon, H., Kürten, A., Almeida, J., Duplissy, J., Williamson, C., Ortega, I. K., Pringle, K. J., Adamov, A., Baltensperger, U.,
320 Barmet, P., Benduhn, F., Bianchi, F., Breitenlechner, M., Clarke, A., Curtius, J., Dommen, J., Donahue, N. M., Ehrhart, S., Flagan, R. C., Franchin, A., Guida, R., Hakala, J., Hansel, A., Heinritzi, M., Jokinen, T., Kangasluoma, J., Kirkby, J., Kulmala, M., Kupc, A., Lawler, M. J., Lehtipalo, K., Makhmutov, V., Mann, G., Mathot, S., Merikanto, J., Miettinen, P., Nenes, A., Onnela, A., Rap, A., Reddington, C. L. S., Riccobono, F., Richards, N. A. D., Rissanen, M. P., Rondo, L., Sarnela, N., Schobesberger, S., Sengupta, K., Simon, M., Sipilä, M., Smith, J. N., Stozkhov, Y., Tomé, A., Tröstl, J., Wagner, P. E., Wimmer, D., Winkler, P. M., Worsnop, D. R., and Carslaw, K. S.: Global
325 Atmospheric Particle Formation from CERN CLOUD Measurements, *Science*, 354, 1119–1124, <https://doi.org/10.1126/science.aaf2649>, 2016.

Ehn, M., Thornton, J. A., Kleist, E., Sipilä, M., Junninen, H., Pullinen, I., Springer, M., Rubach, F., Tillmann, R., Lee, B., and et al.: A Large Source of Low-Volatility Secondary Organic Aerosol, *Nature*, 506, 476–479, 2014.

Elm, J.: An Atmospheric Cluster Database Consisting of Sulfuric Acid, Bases, Organics, and Water, *ACS Omega*, 4, 10965–10974, 2019.

330 Elm, J.: Clusteromics II: Methanesulfonic Acid-Base Cluster Formation, *ACS Omega*, 7, 17035–17044, 2021a.

Elm, J.: Clusteromics I: Principles, Protocols, and Applications to Sulfuric Acid-Base Cluster Formation, *ACS Omega*, 6, 7804–7814, <https://doi.org/10.1021/acsomega.1c00306>, 2021b.

Elm, J.: Clusteromics III: Acid Synergy in Sulfuric Acid-Methanesulfonic Acid-Base Cluster Formation, *ACS Omega*, 6, 15206–15214, 2022.



- 335 Elm, J., Kurtén, T., Bilde, M., and Mikkelsen, K. V.: Molecular Interaction of Pinic Acid with Sulfuric Acid: Exploring the Thermodynamic Landscape of Cluster Growth, *J. Phys. Chem. A*, 118, 7892–7900, <https://doi.org/10.1021/jp503736s>, 2014.
- Elm, J., Myllys, N., and Kurtén, T.: What is Required for Highly Oxidized Molecules to Form Clusters with Sulfuric Acid?, *J. Phys. Chem. A.*, 121, 4578–4587, 2017.
- Elm, J., Hyttinen, N., Lin, J. J., Kurtén, T., and Prisle, N. L.: Strong Even/Odd Pattern in the Computed Gas-Phase Stability of Dicarboxylic
340 Acid Dimers: Implications for Condensation Thermodynamics, *J. Phys. Chem. A*, 123, 9594–9599, 2019.
- Elm, J., Kubečka, J., Besel, V., Jääskeläinen, M. J., Halonen, R., Kurtén, T., and Vehkamäki, H.: Modeling the Formation and Growth of Atmospheric Molecular Clusters: A Review, *J. Aerosol Sci.*, 149, 105 621, <https://doi.org/10.1016/j.jaerosci.2020.105621>, 2020.
- Elm, J., Ayoubi, D., Engsvang, M., Jensen, A. B., Knattrup, Y., Kubečka, J., Bready, C. J., Fowler, V. R., Harold, S. E., Longworth, O. M.,
345 and Shields, G. C.: Quantum Chemical Modeling of Organic Enhanced Atmospheric Nucleation: A Critical Review, *WIREs Comput. Mol. Sci.*, 13, e1662, 2023.
- Engsvang, M., Wu, H., Knattrup, Y., Kubečka, J., Jensen, A. B., and Elm, J.: Quantum Chemical Modeling of Atmospheric Molecular Clusters Involving Inorganic Acids and Methanesulfonic Acid, *Chem. Phys. Rev.*, 4, 031 311, <https://doi.org/10.1063/5.0152517>, 2023.
- Fang, X., Hu, M., Shang, D., Tang, R., Shi, L., Olenius, T., Wang, Y., Wang, H., Zhang, Z., Chen, S., and et al.: Observational Evidence for the Involvement of Dicarboxylic Acids in Particle Nucleation, *Environ. Sci. Technol. Lett.*, 7, 388–394, 2020.
- 350 Glasoe, W. A., Volz, K., Panta, B., Freshour, N., Bachman, R., Hanson, D. R., McMurry, P. H., and Jen, C.: Sulfuric acid Nucleation: An Experimental Study of the Effect of Seven Bases, *J. Geophys. Res. Atmos.*, 120, 1933–1950, <https://doi.org/10.1002/2014JD022730>, 2015.
- Grimme, S., Bannwarth, C., and Shushkov, P.: A Robust and Accurate Tight-Binding Quantum Chemical Method for Structures, Vibrational
355 Theory Comput., 13, 1989–2009, 2017.
- Hallquist, M., Wenger, J. C., Baltensperger, U., Rudich, Y., Simpson, D., Claeys, M., Dommen, J., Donahue, N. M., George, C., Goldstein, A. H., and et al.: The Formation, Properties and Impact of Secondary Organic Aerosol: Current and Emerging Issues, *Atmos. Chem. Phys.*, 9, 5155–5236, 2009.
- He, X.-C., Tham, Y. J., Dada, L., Wang, M., Finkenzeller, H., Stolzenburg, D., Iyer, S., Simon, M., Kürten, A., Shen, J., et al.: Role of Iodine
360 Oxoacids in Atmospheric Aerosol Nucleation, *Science*, 371, 589–595, 2021.
- He, X.-C., Simon, M., Iyer, S., Xie, H.-B., Rörup, B., Shen, J., Finkenzeller, H., Stolzenburg, D., Zhang, R., and Baccharini, A.: Iodine Oxoacids Enhance Nucleation of Sulfuric Acid Particles in the Atmosphere, *Science*, 382, 1308–1314, 2023.
- Henschel, H., Navarro, J. C. A., Yli-Juuti, T., Kupiainen-Määttä, O., Olenius, T., Ortega, I. K., Clegg, S. L., Kurtén, T., Riipinen, I., and Vehkamäki, H.: Hydration of Atmospherically Relevant Molecular Clusters: Computational Chemistry and Classical Thermodynamics, *J.*
365 *Phys. Chem. A*, 118, 2599–2611, <https://doi.org/10.1021/jp500712y>, 2014.
- Hoffmann, T., Odum, J. R., Bowman, F., Collins, D., Klockow, D., Flagan, R. C., and Seinfeld, J. H.: Formation of Organic Aerosols from the Oxidation of Biogenic Hydrocarbons, *J. Atmos. Chem.*, 26, 189–222, <https://doi.org/10.1023/A:1005734301837>, 1997.
- Jaoui, M., Corse, E., Kleindienst, T. E., Offenberg, J. H., Lewandowski, M., and Edney, E. O.: Analysis of Secondary Organic Aerosol Compounds from the Photooxidation of d-Limonene in the Presence of NO_x and their Detection in Ambient PM_{2.5}, *Environ. Sci. Technol.*,
370 40, 3819–3828, 2006.
- Jen, C. N., McMurry, P. H., and Hanson, D. R.: Stabilization of Sulfuric Acid Dimers by Ammonia, Methylamine, Dimethylamine, and Trimethylamine, *J. Geophys. Res. Atmos.*, 119, 7502–7514, <https://doi.org/10.1002/2014JD021592>, 2014.



- Jimenez, J. L., Canagaratna, M. R., Donahue, N. M., Prevot, A. S. H., Zhang, Q., Kroll, J. H., DeCarlo, P. F., Allan, J. D., Coe, H., Ng, N. L., and et al.: Evolution of Organic Aerosols in the Atmosphere, *Science*, 326, 1525–1529, 2009.
- 375 Kenseth, C. M., Hafeman, N. J., Rezugui, S. P., Chen, J., Huang, Y., Dalleska, N. F., Kjaergaard, H. G., Stoltz, B. M., Seinfeld, J. H., and Wennberg, P. O.: Particle-Phase Accretion Forms Dimer Esters in Pinene Secondary Organic Aerosol, *Science*, 382, 787–792, <https://doi.org/10.1126/science.adi0857>, 2023.
- Kirkby, J., Curtius, J., Almeida, J., Dunne, E., Duplissy, J., Ehrhart, S., Franchin, A., Gagne, S., Ickes, L., Kürten, and et al.: Role of Sulphuric Acid, Ammonia and Galactic Cosmic Rays in Atmospheric Aerosol Nucleation, *Nature*, 476, 429–433, 380 <https://doi.org/10.1038/nature10343>, 2011.
- Knattrup, Y. and Elm, J.: Clusteromics IV: The Role of Nitric Acid in Atmospheric Cluster Formation, *ACS Omega*, 7, 31 551–31 560, 2022.
- Kostenidou, E., Karnezi, E., Kolodziejczyk, A., Szmigielski, R., and Pandis, S. N.: Physical and Chemical Properties of 3-Methyl-1,2,3-butanetricarboxylic Acid (MBTCA) Aerosol, *Environ. Sci. Technol.*, 52, 1150–1155, <https://doi.org/10.1021/acs.est.7b04348>, 2018.
- Kristensen, K., Enggrob, K. L., King, S. M., Worton, D. R., Platt, S. M., Mortensen, R., Rosenoern, T., Surratt, J. D., Bilde, M., Goldstein, 385 A. H., and Glasius, M.: Formation and Occurrence of Dimer Esters of Pinene Oxidation Products in Atmospheric Aerosols, *Atmos. Chem. Phys.*, 13, 3763–3776, <https://doi.org/10.5194/acp-13-3763-2013>, 2013.
- Kristensen, K., Watne, A. K., Hammes, J., Lutz, A., Petäjä, T., Hallquist, M., Bilde, M., and Glasius, M.: High-Molecular Weight Dimer Esters Are Major Products in Aerosols from α -Pinene Ozonolysis and the Boreal Forest, *Environ. Sci. Technol. Lett.*, 3, 280–285, <https://doi.org/10.1021/acs.estlett.6b00152>, 2016.
- 390 Kubečka, J.: Developing efficient configurational sampling : structure, formation, and stability of atmospheric molecular clusters, PhD dissertation, University of Helsinki, 2021.
- Kubečka, J., Besel, V., Kurtén, T., Mylly, N., and Vehkamäki, H.: Configurational Sampling of Noncovalent (Atmospheric) Molecular Clusters: Sulfuric Acid and Guanidine, *J. Phys. Chem. A*, 123, 6022–6033, 2019.
- Kubečka, J., Besel, V., Neefjes, I., Knattrup, Y., Kurtén, T., Vehkamäki, H., and Elm, J.: Computational Tools for Handling Molecular 395 Clusters: Configurational Sampling, Storage, Analysis, and Machine Learning, *ACS Omega*, 8, 45 115–45 128, 2023a.
- Kubečka, J., Neefjes, I., Besel, V., Qiao, F., Xie, H.-B., and Elm, J.: Atmospheric Sulfuric Acid–Multi-Base New Particle Formation Revealed through Quantum Chemistry Enhanced by Machine Learning, *J. Phys. Chem. A*, 127, 2091–2103, 2023b.
- Kulmala, M., Kontkanen, J., Junninen, H., Lehtipalo, K., Manninen, H. E., Nieminen, T., Petäjä, T., Sipilä, M., Schobesberger, S., Rantala, P., et al.: Direct Observations of Atmospheric Aerosol Nucleation, *Science*, 339, 943–946, <https://doi.org/10.1126/science.1227385>, 2013.
- 400 Kurtén, T., Loukonen, V., Vehkamäki, H., and Kulmala, M.: Amines are Likely to Enhance Neutral and Ion-Induced Sulfuric Acid-Water Nucleation in the Atmosphere more Effectively than Ammonia, *Atmos. Chem. Phys.*, 8, 4095–4103, <https://doi.org/10.5194/acp-8-4095-2008>, 2008.
- Laj, P., Klausen, J., Bilde, M., Plaß-Duelmer, C., Pappalardo, G., Clerbaux, C., Baltensperger, U., Hjorth, J., Simpson, D., Reimann, S., Coheur, P.-F., Richter, A., De Mazière, M., Rudich, Y., McFiggans, G., Torseth, K., Wiedensohler, A., Morin, S., Schulz, M., 405 Allan, J., Attié, J.-L., Barnes, I., Birmili, W., Cammas, J., Dommen, J., Dorn, H.-P., Fowler, D., Fuzzi, S., Glasius, M., Granier, C., Hermann, M., Isaksen, I., Kinne, S., Koren, I., Madonna, F., Maione, M., Massling, A., Moehler, O., Mona, L., Monks, P., Müller, D., Müller, T., Orphal, J., Peuch, V.-H., Stratmann, F., Tanré, D., Tyndall, G., Abo Riziq, A., Van Roozendael, M., Villani, P., Wehner, B., Wex, H., and Zardini, A.: Measuring atmospheric composition change, *Atmospheric Environment*, 43, 5351–5414, <https://doi.org/https://doi.org/10.1016/j.atmosenv.2009.08.020>, aCCENT Synthesis, 2009.



- 410 Lehtipalo, K., Yan, C., Dada, L., Bianchi, F., Xiao, M., Wagner, R., Stolzenburg, D., Ahonen, L. R., Amorim, A., Baccarini, A., et al.: Multicomponent New Particle Formation from Sulfuric Acid, Ammonia and Biogenic Vapors, *Sci. Adv.*, 4, 1–9, 2018.
- Liakos, D. G., Sparta, M., Kesharwani, M. K., Martin, J. M. L., and Neese, F.: Exploring the Accuracy Limits of Local Pair Natural Orbital Coupled-Cluster Theory, *J. Chem. Theory Comput.*, 11, 1525–1539, 2015.
- Loukonen, V., Kurtén, T., Ortega, I. K., Vehkamäki, H., Pádua, A. A. H., Sellegri, K., and Kulmala, M.: Enhancing Effect of Dimethyl-
415 amine in Sulfuric Acid Nucleation in the Presence of Water – a Computational Study, *Atmos. Chem. Phys.*, 10, 4961–4974, <https://doi.org/10.5194/acp-10-4961-2010>, 2010.
- McGrath, M. J., Olenius, T., Ortega, I. K., Loukonen, V., Paasonen, P., Kurtén, T., Kulmala, M., and Vehkamäki, H.: Atmospheric Cluster Dynamics Code: A Flexible Method for Solution of the Birth-Death Equations, *Atmos. Chem. Phys.*, 12, 2345–2355, 2012.
- Merikanto, J., Spracklen, D. V., Mann, G. W., Pickering, S. J., and Carslaw, K. S.: Impact of Nucleation on Global CCN, *Atmos. Chem. Phys.*, 9, 8601–8616, <https://doi.org/10.5194/acp-9-8601-2009>, 2009.
420
- Metzger, A., Verheggen, B., Dommen, J., Duplissy, J., Prevot, A. S. H., Weingartner, E., Riipinen, I., Kulmala, M., Spracklen, D. V., Carslaw, K. S., and Baltensperger, U.: Evidence for the Role of Organics in Aerosol Particle Formation under Atmospheric Conditions, *Proc. Natl. Acad. Sci. U.S.A.*, 107, 6646–6651, 2010.
- Müller, L., Reinnig, M.-C., Naumann, K. H., Saathoff, H., Mentel, T. F., Donahue, N. M., and Hoffmann, T.: Formation of 3-methyl-1,2,3-
425 butanetricarboxylic Acid via Gas Phase Oxidation of Pinonic Acid – A Mass Spectrometric Study of SOA Aging, *Atmos. Chem. Phys.*, 12, 1483–1496, 2012.
- Nadykto, A. B. and Yu, F.: Strong Hydrogen Bonding between Atmospheric Nucleation Precursors and common Organics, *Chem. Phys. Lett.*, 435, 14–18, <https://doi.org/10.1016/j.cplett.2006.12.050>, 2007.
- Nadykto, A. B., Yu, F., Jakovleva, M. V., Herb, J., and Xu, Y.: Amines in the Earth’s Atmosphere: A Density Functional Theory Study of the
430 Thermochemistry of Pre-Nucleation Clusters, *Entropy*, 13, 554–569, <https://doi.org/10.3390/e13020554>, 2011.
- Nadykto, A. B., Herb, J., Yu, F., and Xu, Y.: Enhancement in the Production of Nucleating Clusters due to Dimethylamine and Large Uncertainties in the Thermochemistry of Amine-Enhanced Nucleation, *Chem. Phys. Lett.*, 609, 42–49, <https://doi.org/10.1016/j.cplett.2014.03.036>, 2014.
- Nadykto, A. B., Herb, J., Yu, F., Xu, Y., and Nazarenko, E. S.: Estimating the Lower Limit of the Impact of Amines on Nucleation in the
435 Earth’s Atmosphere, *Entropy*, 17, 2764–2780, <https://doi.org/10.3390/e17052764>, 2015.
- Neefjes, I., Knattrup, Y., Wu, H., Trolle, G. B., Elm, J., and Kubečka, J.: Thermodynamic Benchmarking of Hydrated Atmospheric Clusters in Early Particle Formation, *Aerosol Research*, 4, 1–22, <https://doi.org/10.5194/ar-4-1-2026>, 2026.
- Neese, F.: Software update: The ORCA program system—Version 5.0, *WIREs Comput. Mol. Sci.*, 12, e1606, 2022.
- Odbadrakh, T. T., Gale, A. G., T., B. B., Temelso, B., and Shields, G. C.: Computation of Atmospheric Concentrations of Molecular Clusters
440 from ab initio Thermochemistry, *J. Vis. Exp.*, 8, e60964, <https://doi.org/10.3791/60964>, 2020.
- O’Dowd, C. D., Jimenez, J. L., Bahreini, R., Flagan, R. C., Seinfeld, J. H., Hämeri, K., Pirjola, L., Kulmala, M., Jennings, S. G., and Hoffmann, T.: Marine Aerosol Formation From Biogenic Iodine Emissions, *Nature*, 417, 632–636, 2002.
- Olenius, T., Kupiainen-Määttä, O., Ortega, I. K., Kurtén, T., and Vehkamäki, H.: Free energy Barrier in the Growth of Sulfuric Acid–Ammonia and Sulfuric Acid–Dimethylamine Clusters, *J. Chem. Phys.*, 139, 084312, <https://doi.org/10.1063/1.4819024>, 2013.
- 445 Pathak, R. K., Stanier, C. O., Donahue, N. M., and Pandis, S. N.: Ozonolysis of α -pinene at atmospherically relevant concentrations: Temperature dependence of aerosol mass fractions (yields), *Journal of Geophysical Research: Atmospheres*, 112, <https://doi.org/https://doi.org/10.1029/2006JD007436>, 2007.



- Pedersen, A. N., Knattrup, Y., and Elm, J.: A cluster-of-functional-groups approach for studying organic enhanced atmospheric cluster formation, *Aerosol Research*, 2, 123–134, <https://doi.org/10.5194/ar-2-123-2024>, 2024.
- 450 Peräkylä, O., Berndt, T., Franzon, L., Hasan, G., Meder, M., Valiev, R. R., Daub, C. D., Varelas, J. G., Geiger, F. M., Thomson, R. J., Rissanen, M., Kurtén, T., and Ehn, M.: Large Gas-Phase Source of Esters and Other Accretion Products in the Atmosphere, *Journal of the American Chemical Society*, 145, 7780–7790, <https://doi.org/10.1021/jacs.2c10398>, PMID: 36995167, 2023.
- Pracht, P., Bohle, F., and Grimme, S.: Automated Exploration of the Low-Energy Chemical Space With Fast Quantum Chemical Methods, *Phys. Chem. Chem. Phys.*, 22, 7169–7192, <https://doi.org/10.1039/C9CP06869D>, 2020.
- 455 Quéléver, L. L. J., Kristensen, K., Normann Jensen, L., Rosati, B., Teiwes, R., Daellenbach, K. R., Peräkylä, O., Roldin, P., Bossi, R., Pedersen, H. B., Glasius, M., Bilde, M., and Ehn, M.: Effect of temperature on the formation of highly oxygenated organic molecules (HOMs) from alpha-pinene ozonolysis, *Atmospheric Chemistry and Physics*, 19, 7609–7625, <https://doi.org/10.5194/acp-19-7609-2019>, 2019.
- Rasmussen, F. R., Kubečka, J., Besel, V., Vehkamäki, H., Mikkelsen, K. V., Bilde, M., and Elm, J.: Hydration of Atmospheric Molecular Clusters III: Procedure for Efficient Free Energy Surface Exploration of Large Hydrated Clusters, *J. Phys. Chem. A*, 124, 5253–5261, <https://doi.org/10.1021/acs.jpca.0c02932>, 2020.
- 460 Riccobono, F., Schobesberger, S., Scott, C. E., Dommen, J., Ortega, I. K., Rondo, L., Almeida, J., Amorim, A., Bianchi, F., Breitenlechner, M., and et al.: Oxidation Products of Biogenic Emissions Contribute to Nucleation of Atmospheric Particles, *Science*, 344, 717–721, 2014.
- Riplinger, C. and Neese, F.: An Efficient and Near Linear Scaling Pair Natural Orbital Based Local Coupled Cluster Method, *J. Chem. Phys.*, 138, 034 106, 2013.
- 465 Riplinger, C., Sandhoefer, B., Hansen, A., and Neese, F.: Natural Triple Excitations in Local Coupled Cluster Calculations With Pair Natural Orbitals, *J. Chem. Phys.*, 139, 134 101, 2013.
- Schobesberger, S., Junninen, H., Bianchi, F., Lönn, G., Ehn, M., Lehtipalo, K., Dommen, J., Ehrhart, S., Ortega, I. K., Franchin, A., and et al.: Molecular Understanding of Atmospheric Particle Formation from Sulfuric Acid and Large Oxidized Organic Molecules, *Proc. Natl. Acad. Sci. U.S.A.*, 110, 17 223–17 228, <https://doi.org/10.1073/pnas.1306973110>, 2013.
- 470 Simon, M., Dada, L., Heinritzi, M., Scholz, W., Stolzenburg, D., Fischer, L., Wagner, A. C., Kürten, A., Rörup, B., He, X.-C., and et al.: Molecular Understanding of New-particle Formation from α -pinene between -50 and $+25$ °C, *Atmos. Chem. Phys.*, 20, 9183–9207, 2020.
- Sipilä, M., Berndt, T., Petäjä, T., Brus, D., Vanhanen, J., Stratmann, F., Patokoski, J., Mauldin, R. L., Hyvärinen, A.-P., Lihavainen, H., and Kulmala, M.: The Role of Sulfuric Acid in Atmospheric Nucleation, *Science*, 327, 1243–1246, 2010.
- 475 Sipilä, M., Sarnela, N., Jokinen, T., Henschel, H., Junninen, H., Kontkanen, J., Richters, S., Kangasluoma, J., Franchin, A., Peräkylä, O., and et al.: Molecular-scale Evidence of Aerosol Particle Formation Via Sequential Addition of HIO₃, *Nature*, 537, 532–534, 2016.
- Tan, S., Chen, X., and Yin, S.: Comparison Results of Eight Oxygenated Organic Molecules: Unexpected Contribution to New Particle Formation in the Atmosphere, *Atmos. Environ.*, 268, 118 817, 2022.
- 480 Temelso, B., Morrell, T. E., Shields, R. M., Allodi, M. A., Wood, E. K., Kirschner, K. N., Castonguay, T. C., Archer, K. A., and Shields, G. C.: Quantum Mechanical Study of Sulfuric Acid Hydration: Atmospheric Implications, *J. Phys. Chem. A*, 116, 2209–2224, <https://doi.org/10.1021/jp2119026>, 2012a.
- Temelso, B., Phan, T. N., and Shields, G. C.: Computational Study of the Hydration of Sulfuric Acid Dimers: Implications for Acid Dissociation and Aerosol Formation, *J. Phys. Chem. A*, 116, 9745–9758, <https://doi.org/10.1021/jp3054394>, 2012b.



- 485 Temelso, B., Morrison, E. F., Speer, D. L., Cao, B. C., Appiah-Padi, N., Kim, G., and Shields, G. C.: Effect of Mixing Ammonia and Alkylamines on Sulfate Aerosol Formation, *J. Phys. Chem. A*, 122, 1612–1622, 2018.
- Thomsen, D., Elm, J., Rosati, B., Skønager, J. T., Bilde, M., and Glasius, M.: Large Discrepancy in the Formation of Secondary Organic Aerosols from Structurally Similar Monoterpenes, *ACS Earth Space Chem.*, 5, 632–644, 2021.
- Thomsen, D., Thomsen, L. D., Iversen, E. M., Björgvinsdóttir, T. N., Vinther, S. F., Skønager, J. T., Hoffmann, T., Elm, J., Bilde, M., and
490 Glasius, M.: Ozonolysis of α -Pinene and Δ^3 -Carene Mixtures: Formation of Dimers with Two Precursors, *Environ. Sci. Technol.*, 56, 16 643–16 651, 2022.
- Thomsen, D., Iversen, E. M., Skønager, J. T., Luo, Y., Li, L., Roldin, P., Priestley, M., Pedersen, H. B., Hallquist, M., Ehn, M., et al.: The Effect of Temperature and Relative Humidity on Secondary Organic Aerosol Formation from Ozonolysis of Δ^3 -carene, *Environ. Sci.: Atmos.*, 4, 88–103, 2024.
- 495 Wang, Z.-Q., Liu, Y.-R., Wang, C.-Y., Jiang, S., Feng, Y.-J., Huang, T., and Huang, W.: Multicomponent nucleation of malonic acid involved in the sulfuric acid - dimethylamine system and its atmospheric implications, *Atmos. Environ.*, 267, 118 558, <https://doi.org/https://doi.org/10.1016/j.atmosenv.2021.118558>, 2021.
- Weber, R. J., Marti, J. J., McMurry, P. H., Eisele, F. L., Tanner, D. J., and Jefferson, A.: Measured Atmospheric New Particle Formation Rates: Implications for Nucleation Mechanisms, *Chem. Eng. Commun.*, pp. 53–64, [https://www.tandfonline.com/doi/abs/10.1080/](https://www.tandfonline.com/doi/abs/10.1080/00986449608936541)
500 00986449608936541, 1996.
- Yasmeen, F., Szmigielski, R., Vermeylen, R., Gómez-González, Y., Surratt, J. D., Chan, A. W. H., Seinfeld, J. H., Maenhaut, W., and Claeys, M.: Mass Spectrometric Characterization of Isomeric Terpenoic Acids From the Oxidation of α -pinene, β -pinene, d-limonene, and Δ^3 -carene in Fine Forest Aerosol, *J. Mass Spectrom.*, 46, 425–442, 2011.
- Zhang, H., Li, H., Liu, L., Zhang, Y., Zhang, X., and Li, Z.: The potential role of malonic acid in the atmospheric sulfuric acid - Ammonia
505 clusters formation, *Chemosphere*, 203, 26–33, <https://doi.org/https://doi.org/10.1016/j.chemosphere.2018.03.154>, 2018.
- Zhang, J. and Dolg, M.: ABCluster: The Artificial Bee Colony Algorithm for Cluster Global Optimization, *Phys. Chem. Chem. Phys.*, 17, 24 173–24 181, 2015.
- Zhang, R., Suh, I., Zhao, J., Zhang, D., Fortner, E. C., Tie, X., Molina, L. T., and Molina, M. J.: Atmospheric New Particle Formation Enhanced by Organic Acids, *Science*, 304, 1487–1490, 2004.
- 510 Zhang, R., Wang, L., Khalizov, A. F., Zhao, J., Zheng, J., McGraw, R. L., and Molina, L. T.: Formation of Nanoparticles of Blue Haze Enhanced by Anthropogenic Pollution, *Proc. Natl. Acad. Sci. U.S.A.*, 106, 17 650–17 654, 2009.
- Zhao, B., Donahue, N. M., Zhang, K., Mao, L., Shrivastava, M., Ma, P.-L., Shen, J., Wang, S., Sun, J., Gordon, H., and et al.: Global Variability in Atmospheric New Particle Formation mechanisms, *Nature*, 631, 98–105, <https://doi.org/10.1038/s41586-024-07547-1>, 2024.